Multiple Novel Modes of Action Involved in the *In Vitro* Neurotoxic Effects of Tetrabromobisphenol-A

Hester S. Hendriks, Regina G. D. M. van Kleef, Martin van den Berg, and Remco H. S. Westerink[1]

Neurotoxicology Research Group, Toxicology Division, Institute for Risk Assessment Sciences (IRAS), Utrecht University, NL-3508 TD Utrecht, The Netherlands

[1]To whom correspondence should be addressed at Neurotoxicology Research Group, Toxicology Division, Institute for Risk Assessment Sciences (IRAS), Utrecht University, PO Box 80.177, NL-3508 TD Utrecht, The Netherlands. Fax: +31-30-2535077. E-mail: r.westerink@uu.nl.

Neurotoxicological data on the widely used brominated flame retardant tetrabromobisphenol-A (TBBPA) is limited. Since recent studies indicated that inhibitory $GABA_A$ and excitatory $\alpha_4\beta_2$ nicotinic acetylcholine (nACh) receptors are sensitive targets for persistent organic pollutants, we investigated the effects of TBBPA on these receptors, expressed in *Xenopus* oocytes, using the two-electrode voltage-clamp technique. Our results demonstrate that TBBPA acts as full ($\geq 10\mu M$) and partial ($\geq 0.1\mu M$) agonist on human $GABA_A$ receptors, whereas it acts as antagonist ($\geq 10 \mu M$) on human $\alpha_4\beta_2$ nACh receptors. Next, neuronal B35 cells were used to further study the effects of TBBPA on calcium-permeable nACh receptors using single-cell fluorescent calcium imaging. These results demonstrate that TBBPA ($\geq 1\mu M$) inhibits acetylcholine (ACh) receptors as evidenced by a reduction in the ACh-evoked increases in the intracellular calcium concentration ($[Ca^{2+}]_i$). Additionally, TBBPA ($> 1\mu M$) induced a strong and concentration-dependent increase in basal $[Ca^{2+}]_i$ in B35 cells. Similarly, TBBPA ($> 1\mu M$) increases basal $[Ca^{2+}]_i$ in dopaminergic PC12 cells. This increase is also evident under calcium-free conditions, indicating it originates from intracellular calcium stores. Moreover, depolarization-evoked increases in $[Ca^{2+}]_i$ are strongly reduced by TBBPA ($\geq 1\mu M$), indicating TBBPA-induced inhibition of voltage-gated calcium channels. Our *in vitro* studies thus demonstrate that TBBPA exerts several adverse effects on functional neurotransmission endpoints with effect concentrations that are only two orders of magnitude below the highest cord serum concentrations. Although epidemiological proof for adverse TBBPA effects is lacking, our data justify the quest for flame retardants with reduced neurotoxic potential.

Key Words: brominated flame retardants; *in vitro* neurotoxicology; human nicotinic acetylcholine receptors; human $GABA_A$ receptors; Ca^{2+}-homeostasis; cell viability.

Tetrabromobisphenol-A (TBBPA) is a widely used brominated flame retardant (BFR) in electrical and electronic equipment such as TVs, computers, printers, cell phones, etc. with an estimated annual worldwide market demand of > 120,000 tons (de Wit *et al.*, 2010). It has been used as a replacement for polybrominated diphenyl ethers (PBDEs), whose persistence in the environment and potential for adverse health effects have prompted concerns (for review, see Dingemans *et al.*, 2011). As TBBPA is a phenolic compound primarily used as a chemically bound flame retardant, it was not expected to reach the environment in large amounts. However, several studies have shown that TBBPA can leak into the environment from treated products (Sellstrom and Jansson, 1995), and recent reports have shown its presence in wildlife and human samples (Covaci *et al.*, 2009; de Wit *et al.*, 2010). The presence of TBBPA in seafood (World Health Organization, 1995) as well as in commercial drinking water that was stored in polycarbonate containers (Peterman *et al.*, 2000) may also contribute to the levels seen in human serum. TBBPA levels have been reported in human serum samples (0.40–0.71 ng/g lw; Thomsen *et al.*, 2002) and adipose tissue samples (0.048 ng/g lw; Johnson-Restrepo *et al.*, 2008) of nonoccupationally exposed adults. Following analysis of house dust samples in Germany and the United States, the daily exposure for toddlers was estimated to be 0.2 ng/kg bw/d for TBBPA (Abb *et al.*, 2011). The daily exposure of a 1-month-old infant via breast milk was estimated to be as high as 1 ng/kg bw/d (Abdallah and Harrad, 2011). Because the usage of TBBPA in Asia is about eight times higher than in Europe (Law *et al.*, 2006), values for human serum samples as well as dust samples are at least a factor of three higher in Asia (Nagayama *et al.*, 2000; Takigami *et al.*, 2009).

Although PBDEs are clearly associated with neurotoxicity (for review, see Dingemans *et al.*, 2011), information on the neurotoxicity of TBBPA is limited. It has been demonstrated that neonatal TBBPA exposure does not result in behavioral effects in adult mice (Eriksson *et al.*, 2001) but can affect the cholinergic system in neonates (Viberg and Eriksson, 2011). Moreover, behavioral effects in mice following acute exposure to TBBPA have been reported (Nakajima *et al.*, 2009). Additionally, TBBPA was shown to concentration dependently increase the production of reactive oxygen species (ROS) *in vitro* (Reistad *et al.*, 2005, 2007). Furthermore, at low micromolar concentrations TBBPA increases the basal intracellular calcium concentration ($[Ca^{2+}]_i$), extracellular glutamate levels, and cell

death in human neutrophil granulocytes and cerebellar granule cells (Reistad *et al.*, 2005, 2007). In Sertoli cells, TBBPA induces apoptosis via increases in $[Ca^{2+}]_i$ involving Ca^{2+}-dependent mitochondrial depolarization, inhibition of sarcoplasmic/endoplasmic reticulum (ER) Ca^{2+}-ATPases and activation of ryanodine receptor Ca^{2+}-channels (Ogunbayo *et al.*, 2008). These findings are of importance as Ca^{2+} plays an essential role in multiple physiological and pathological processes, including neurotransmission (Garcia *et al.*, 2006; Westerink, 2006) and cell viability (Orrenius *et al.*, 2011).

So far, most studies on the *in vitro* neurotoxic potential of TBBPA focused on cytotoxicity or presynaptic effects of neurotransmission, although recent studies indicate that persistent organic pollutants (POPs), such as PBDEs and polychlorinated biphenyls (PCBs), can also affect postsynaptic human $GABA_A$ and $\alpha_4\beta_2$ nicotinic acetylcholine (nACh) receptors (Antunes Fernandes *et al.*, 2010; Hendriks *et al.*, 2010). The $GABA_A$ receptor is the main inhibitory neurotransmitter receptor in the central nervous system, whereas the $\alpha_4\beta_2$ nACh receptor is an abundant excitatory neurotransmitter receptor in the central and peripheral nervous system. Both receptors are also critically involved in brain development as well as in long-term potentiation and synaptic plasticity (Dwyer *et al.*, 2009; D'Hulst *et al.*, 2009). Possible effects of TBBPA on these receptors are thus of considerable interest.

In the present study, we investigated the acute effects of TBBPA on human $GABA_A$ and $\alpha_4\beta_2$ nACh receptors, expressed in *Xenopus* oocytes, using the two-electrode voltage-clamp technique. To further unravel the mechanisms underlying the observed changes in neuronal signaling, B35 neuroblastoma cells were used to investigate the acute effects of TBBPA on Ca^{2+}-homeostasis and acetylcholine (ACh)-evoked increases in $[Ca^{2+}]_i$. Although B35 cells lack functional voltage-gated calcium channels (VGCCs), these cells have proven to be useful in the molecular analysis of endocytosis and intra- and intercellular signaling pathways (Otey *et al.*, 2003), including ACh-mediated signaling (Heusinkveld and Westerink, 2011), due to their high expression of calcium-permeable nACh receptors. Dopaminergic pheochromocytoma (PC12) cells, which are widely used to assess neurotoxicity, neuronal function, and calcium homeostasis (for review, see Westerink and Ewing, 2008), were used to study in more detail the observed effects of this BFR on basal and depolarization-evoked calcium homeostasis.

MATERIALS AND METHODS

Chemicals. $CaCl_2$ (1M solution), $MgCl_2$ (1M solution), $MgSO_4$, $NaHCO_3$, NaOH, $Ca(NO_3)_2$, KCl, glucose, sucrose, and 4-(2-hydroxyethyl)-1-piperazineethanesulfonic acid (HEPES) were purchased from Merck (Darmstadt, Germany). RPMI 1640, DMEM, PenStrep, PBS, Fura-2 AM, and 2′,7′-dichlororfluorescin diacetate (H_2-DCFDA) were obtained from Invitrogen (Breda, The Netherlands). All other chemicals were obtained from Sigma-Aldrich (Zwijndrecht, The Netherlands), unless otherwise noted. Saline

solutions for measurements of $[Ca^{2+}]_i$ and production of ROS were prepared with deionized water (Milli-Q; resistivity > 10 M$\Omega \times$ cm) and contained (in millimolar) 125 NaCl, 5.5 KCl, 2 $CaCl_2$, 0.8 $MgCl_2$, 10 HEPES, 24 glucose, and 36.5 sucrose (pH 7.3 with NaOH). Saline solutions for oocyte electrophysiology contained (in millimolar) 115 NaCl, 2.5 KCl, 1 $CaCl_2$, and 10 HEPES (pH 7.2 with NaOH). Stock solutions of 2mM ionomycin in dimethyl sulfoxide (DMSO) were kept at $-20°C$. Gabazine (SR-95531) stock solution of 100mM in DMSO was further diluted to obtain an experimental concentration of 25µM. Stock solutions of 0.1–100mM TBBPA ($> 99\%$ pure, Sigma-Aldrich) were prepared in DMSO and diluted in saline to obtain the desired concentrations just prior to the experiments (all solutions used in experiments, including control experiments, contained 0.1% DMSO). All experiments were performed at room temperature (20°C–22°C).

Electrophysiological recordings of $\alpha_1\beta_2\gamma_2$ $GABA_A$ or $\alpha_4\beta_2$ nicotinic ACh receptors function in* Xenopus laevis *oocytes. All procedures have been described previously (Hendriks *et al.*, 2010) and were conducted in accordance with Dutch law and approved by the Ethical Committee for Animal Experiments of Utrecht University. Briefly, adult female *Xenopus laevis* (provided by Dr Wim Scheenen, Radboud University, Nijmegen, The Netherlands) were anesthetized by submersion in 0.1% MS-222, and ovarian lobes were surgically removed. Oocytes were treated with collagenase type I (1.5 mg/ml Ca^{2+}-free Barth's solution) for 90 min at room temperature before manual defolliculation. Complementary DNA (cDNA) coding for the human α_1, β_2, and γ_2 subunits of human $GABA_A$ receptors (Origene, Rockville, MD) was dissolved in distilled water at a 1:1:1 molar ratio and injected (23 nl/oocyte, ~1 ng of each subunit) into the nuclei of stage V or VI oocytes using a Nanoject Automatic Oocyte Injector (Drummond, Broomall, PA). cDNA coding for the human α_4 and β_2 subunits of the human neuronal nicotinic acetylcholine receptors (kindly provided by Janssen Pharmaceutica N.V., Beerse, Belgium) was dissolved in distilled water at a 1:1 molar ratio and injected in a total injection volume of 18.4 nl/oocyte (~0.2 ng of each subunit). Sham-injected oocytes were injected with 23 or 18.4 nl distilled water, i.e., without cDNA. Following injection with cDNA or distilled water, oocytes were incubated at 21°C in modified Barth's solution containing (in millimolar) 88 NaCl, 1 KCl, 2.4 $NaHCO_3$, 0.3 $Ca(NO_3)_2$, 0.41 $CaCl_2$, 0.82 $MgSO_4$, 15 HEPES, and 10 µg/ml neomycin (pH 7.6 with NaOH).

Electrophysiological experiments were performed on oocytes after 2–5 days of incubation to ensure sufficient translation of injected cDNA and functional expression of $\alpha_1\beta_2\gamma_2$ $GABA_A$ or $\alpha_4\beta_2$ nACh receptors in the membrane. Ion currents associated with $GABA_A$ or $\alpha_4\beta_2$ nACh receptor activity were measured with the two-electrode voltage-clamp technique using a Gene Clamp 500B amplifier (Axon Instruments, Union City, CA) with high-voltage output stage as described previously (Hendriks *et al.*, 2010). Recording microelectrodes (0.5–2.5 MΩ) were filled with KCl (3M). Oocytes, placed in a custom-built Teflon oocyte recording chamber, were voltage-clamped at -60 mV and continuously superfused (~30 ml/min) with saline. Membrane currents were low-pass filtered (8-pole Bessel; 3 dB at 0.3 kHz), digitized (12 bits; 1024 samples per record), and stored on disk for computer analysis.

Aliquots of freshly thawed stock solutions of GABA or ACh in distilled water and TBBPA and gabazine in DMSO were added to the saline immediately before the experiments. Oocytes were exposed by switching the perfusate from saline to TBBPA- and/or GABA or ACh-containing saline using a servomotor-operated valve. Oocytes were repeatedly exposed to different GABA or ACh- and/or TBBPA-containing solutions for 20–40 s. For specific experiments, $GABA_A$ receptor expressing oocytes were exposed to a mixture of TBBPA (10µM) and gabazine (25µM). A washout period of 2–5 min between each application was introduced, allowing receptors to recover from desensitization. Sham-injected oocytes did not show any ion current upon superfusion with saline containing 1mM GABA, 1mM ACh, and/or 100µM TBBPA (data not shown). To minimize adsorption of TBBPA to the perfusion system, glass reservoirs and Teflon tubes (polytetrafluoroethylene; 4×6 mm, Rubber, Hilversum, The Netherlands) were used.

Cell culture. B35 rat neuroblastoma cells (Otey *et al.*, 2003) were grown for maximal 10 passages in DMEM medium supplemented with 10% fetal calf

serum (ICN Biomedicals, Zoetermeer, The Netherlands), 1% additional amino acids (stock solution containing 40mM of L-Cys, L-Ala, L-Asp, L-Pro, L-Glu, and L-Asx), 100 U/ml penicillin, and 100 mg/ml streptomycin as described previously (Heusinkveld and Westerink, 2011).

PC12 rat pheochromocytoma cells (Greene and Tischler, 1976) were grown for a maximum of 10 passages in RPMI 1640 medium supplemented with 5% fetal calf serum, 10% horse serum (ICN Biomedicals,), 100 U/ml penicillin, and 100 mg/ml streptomycin as described previously (Hondebrink *et al.*, 2011a).

Cells were grown in a humidified incubator at 37°C and 5% CO_2 and subcultured 1 day prior to measurements of $[Ca^{2+}]_i$, cell viability, or ROS production. For fluorescent microscopy Ca^{2+} imaging experiments, undifferentiated B35 or PC12 (both $1.4 \cdot 10^6$ cells per dish) cells were subcultured in glass-bottom dishes (MatTek, Ashland, MA). For measurements of cell viability or ROS production, undifferentiated B35 or PC12 cells were seeded in 96-well plates (Greiner Bio-one, Solingen, Germany) at a density of 2×10^5 and 1.5×10^5 cells per well, respectively. All culture flasks, dishes, and plates were coated with poly-L-lysine (50 μg/ml).

Single-cell fluorescent $[Ca^{2+}]_i$ imaging. $[Ca^{2+}]_i$ was measured using the Ca^{2+}-sensitive fluorescent ratio dye Fura-2 AM as described previously (Heusinkveld *et al.*, 2010; Hondebrink *et al.*, 2011a). Briefly, B35 or PC12 cells were loaded with 5μM Fura-2 AM for 20 min at room temperature, followed by 15-min de-esterification. After de-esterification, the cells were placed on the stage of an inverted microscope (Zeiss, Göttingen, Germany) equipped with a TILL Photonics Polychrome IV (TILL Photonics GmBH, Gräfelfing, Germany). Fluorescence, evoked by 340 and 380 nm excitation wavelengths (F_{340} and F_{380}), was collected every 6 s at 510 nm with an Image SensiCam digital camera (TILL Photonics GmBH). Changes in F_{340}/F_{380} ratio (R), reflecting changes in $[Ca^{2+}]_i$, were analyzed using custom-made MS-Excel macros.

Cells were continuously superfused (~0.6 ml/min) with saline using a valvelink 8.2 (Automate Scientific, CA). Each experiment consisted of a 5-min baseline recording to measure basal $[Ca^{2+}]_i$, after which an increase in $[Ca^{2+}]_i$ was triggered by switching superfusion for 15 s to saline containing 100μM ACh (B35 cells) or saline containing 100mM K^+ (PC12 cells) to measure stimulation-evoked $[Ca^{2+}]_i$. Following this first stimulation and a 5- to 10-min recovery period, cells were exposed to saline-containing DMSO (0.1%) or TBBPA (0.1–10μM) for 20 min prior to a second stimulation. For specific experiments, the exposure duration was increased from 20 to 40 min. A subset of experiments was performed without superfusion; after 5 min of baseline recording the cells were exposed for 20 min to TBBPA via bath application and subsequently stimulated with ACh or K^+. For mechanistic experiments, cells were washed with Ca^{2+}-free saline (containing 10μM EDTA to remove residual extracellular Ca^{2+}) just prior to the imaging experiments. Where applicable, intracellular Ca^{2+} stores were emptied by incubation for 10 min with 1μM thapsigargin (TG) and 1μM carbonyl cyanide 4-(trifluoromethoxy)phenylhydrazone (FCCP) in Ca^{2+}-free saline as described previously (Dingemans *et al.*, 2008).

Maximum and minimum ratios (R_{max} and R_{min}) were determined at the end of the recording by addition of ionomycin (5μM) and ethylenediamine tetraacetic acid (EDTA; 17mM). Free cytosolic $[Ca^{2+}]_i$ was calculated using a modified Grynkiewicz's equation: $[Ca^{2+}]_i = K_d \times (R - R_{min})/(R_{max} - R)$, where K_d is the dissociation constant of Fura-2 AM determined in the experimental setup (Deitmer and Schild, 2000). The amplitude of the TBBPA-induced increase in basal $[Ca^{2+}]_i$ was determined to quantify the effects of TBBPA on basal $[Ca^{2+}]_i$. The amplitude of the second K^+- or ACh-evoked increase in $[Ca^{2+}]_i$ (after 20 min of exposure to DMSO or TBBPA) was expressed as a percentage of the amplitude of the first stimulation-evoked increase in $[Ca^{2+}]_i$ per cell to obtain a "treatment ratio" (TR) as indicated in Figure 3A and Figure 4A. As persistent changes in basal $[Ca^{2+}]_i$ can influence the amplitude of the stimulation-evoked increase in $[Ca^{2+}]_i$, a net stimulation-evoked increase in $[Ca^{2+}]_i$ was calculated by subtracting the amplitude of $[Ca^{2+}]_i$ just prior to stimulation from the amplitude of the stimulation-evoked increase in $[Ca^{2+}]_i$. Net increases in stimulation-evoked increases in $[Ca^{2+}]_i$ were used to derive a "net TR" as described previously (Hondebrink *et al.*, 2011a; Langeveld *et al.*, 2012).

Cell viability, ROS, and caspase activation assay. To exclude that results are confounded by acute TBBPA-induced cytotoxicity, effects of TBBPA on cell viability in B35 and PC12 cells were determined using a combined alamarBlue (AB) and Neutral Red (NR) assay as described previously (Heusinkveld *et al.*, 2010). The AB assay, which is based on the ability of the cells to reduce resazurin to resorufin, records mitochondrial activity of the cells as a measure of cell viability. Membrane integrity and lysosomal activity were subsequent determined in the NR assay as an independent measure of cell viability. Briefly, following 24-h exposure to TBBPA (1–100μM) in serum-free medium, cells were incubated for 30 min with 200 μl resazurin solution (12μM in PBS) after which resorufin was measured spectrophotometrically at 530/590 nm (excitation/emission; FLUOstar Galaxy V4.30-0, BMG Labtechnologies, Offenburg, Germany). After removal of the AB solution, cells were incubated for 1 h with 200 μl NR solution (12μM in PBS). Following the incubation, cells were rinsed with warm (37°C) PBS, and 100-μl extraction solution (1% glacial acetic acid, 50% ethanol, and 49% H_2O) was added to the wells. After 30-min extraction, fluorescence was measured spectrophotometrically at 430/480 nm (excitation/emission).

ROS production was assessed using the fluorescent dye H_2-DCFDA as described previously (Heusinkveld *et al.*, 2010). Briefly, B35 or PC12 cells seeded in black glass-bottom 96-well plates (Greiner Bio-one) were loaded with 1.5μM H_2-DCFDA for 30 min at 37°C. Subsequently, cells were exposed for up to 24 h to TBBPA-containing saline (1–100μM). ROS production was measured spectrophotometrically as an increase in fluorescence at 485/530 nm (excitation/emission; FLUOstar Galaxy V4.30-0, BMG Labtechnologies).

Effects of TBBPA on activation of caspase-3 were determined using the Casp3F kit (Sigma-Aldrich) according to the manufacturer's instructions. Briefly, PC12 cells were seeded in 24-wells plates at a density of ~4.5 × 10^5 cells per well and exposed to TBBPA (0.1–100μM) for 24 h in serum-free medium. Staurosporine (STS) exposure (1μM) was included as a positive control for caspase-3 induction. Following exposure, cells were exposed to lysis buffer for 15 min on ice, and subsequently, a triplicate of the cell lysate was transferred to a black clear-bottom 96-wells plate. The samples were incubated with 16μM caspase-3 substrate (acetyl Asp-Glu-Cal-Asp 7-amido-4-methylcoumarin) for 45 min at 37°C, and after hydrolysis, cleaved substrate was measured spectrophotometrically at 360/460 nm. To correct the measured fluorescence for cell number, the protein content of the sample was measured using a fluorescamine-based assay (Udenfriend *et al.*, 1972).

Data analysis and statistics. All data are presented as mean ± SEM from the number of wells, cells, or oocytes (n) indicated, derived from 3 to 11 independent experiments (N).

The percentage of TBBPA-induced potentiation of inhibition of the GABA- or ACh-evoked ion current was calculated from the quotient of the maximum amplitude of the GABA- or ACh-TBBPA coapplication response and the maximum amplitude of the control (GABA or ACh) response.

Cells exposed to only DMSO were used as control (set at 100%) and effects of TBBPA on $[Ca^{2+}]_i$ concentrations, cell viability or ROS formation are expressed as percentage of control. Effects on cell viability < 15% were considered irrelevant. For calcium-imaging experiments, the variation within the dish (i.e., between cells) is larger than the variation between the dishes. The individual cells (n) rather than the different dishes (N) are thus the source of variation indicating that statistically all cells are derived from the same population. Additionally, using the dish (N) as statistical unit rather than the cells (n) reduces the possibility to study single-cell calcium kinetics and oscillations. We therefore used the cells (n) rather than the dish (N) as statistical unit for experiments with single-cell resolution (see also Heusinkveld and Westerink, 2012).

Cells or wells that showed effects two times SD above or below average were considered outliers and excluded from further analysis of calcium homeostasis, cell viability, or ROS production. As the SD for the TR in control cells amounted to ~21%, effects on basal $[Ca^{2+}]_i$ and stimulation-evoked TR < 25% were considered irrelevant. Because control cells show basal ROS production over time, these data are expressed as average percentage compared with the time-matched control values. All relevant effects are statistically significant ($p < 0.05$; Student's *t*-test, paired or unpaired where applicable).

The concentration-depended effects of TBBPA were determined by one-way ANOVA and post hoc Bonferroni tests. A p value of < 0.05 was considered statistically significant. Concentration-response curves were calculated using GraphPad Prism version 4.00 (GraphPad Software, San Diego, CA).

RESULTS

Agonistic Effects of TBBPA on Human $\alpha_1\beta_2\gamma_2$ GABA$_A$ Receptor

Voltage-clamped (-60 mV) oocytes expressing $\alpha_1\beta_2\gamma_2$ GABA$_A$ receptors were exposed to different GABA concentrations (0.1μM–3 mM; see Supplementary figure S1 for example recordings). GABA-evoked ion currents were normalized to the response obtained with 1mM GABA and plotted against the agonist concentration to obtain a concentration-effect curve according to the Hill equation. This curve was used to determine the concentrations producing 20 and 50% of the maximal response (EC$_{20}$ and EC$_{50}$). EC$_{20}$, EC$_{50}$, and Hill slope amounted 14μM, 40μM, and 1.20 ± 0.16, respectively ($n = 9$; Supplementary figure S1), which is in line with previous results (Hendriks et al., 2010; Hondebrink et al., 2011b).

To investigate whether TBBPA is able to activate the human GABA$_A$ receptor, GABA responsive oocytes were superfused with saline containing 0.1–10μM TBBPA ($n = 4–5$ oocytes/concentration). Superfusion with 1μM TBBPA resulted in a very small, not significant, activation of the GABA$_A$ receptor, whereas superfusion with 10μM TBBPA resulted in a significant activation of the GABA$_A$ receptor ($8 \pm 1\%$; $p < 0.001$; normalized to the current observed at 1mM GABA; Figs. 1A and B). The kinetics of the observed effect are slow and not completely saturated during the application time (40 s).

Next, TBBPA was coappled with a low-concentration GABA (EC$_{20}$) to determine possible partial agonistic effects, as demonstrated previously for PCBs and PBDEs (Hendriks et al., 2010). At this low receptor occupancy, TBBPA induced a concentration-dependent potentiation of the GABA-induced ion current (Figs. 1A and C). Although a modest potentiation ($26 \pm 3\%$; $p < 0.05$; normalized to the current observed at GABA EC$_{20}$) was observed for 0.1μM TBBPA, a very strong potentiation of the GABA$_A$ receptor was observed after coapplication with 1 or 10μM TBBPA ($210 \pm 33\%$; $p < 0.001$ and $703 \pm 93\%$; $p < 0.001$, respectively). These results indicate that TBBPA acts both as partial and full agonist of the GABA$_A$ receptor with lowest observed effect concentrations (LOECs) of 0.1 and 10μM, respectively.

Pharmacologically blocking the GABA-binding sites of the GABA$_A$ receptor using gabazine (25μM) completely abolished the GABA-evoked current (Supplementary figure S2A), whereas gabazine only partly blocked the TBBPA-induced effect on the GABA$_A$ receptor (Supplementary figure S2B). Because no response was observed in sham-injected oocytes, these combined results indicate that the effect of TBBPA is a direct GABA$_A$ receptor–mediated effect that at least partly involves the GABA-binding sites of the GABA$_A$ receptor.

Antagonistic Effects of TBBPA on Human $\alpha_4\beta_2$ Nicotinic Acetylcholine Receptor

Oocytes expressing human $\alpha_4\beta_2$ nACh receptors were voltage-clamped (-60 mV) and superfused with various concentrations of ACh (0.1μM–3mM; see Supplementary figure S3 for example recordings). ACh-evoked ion currents were normalized to the response obtained with 1mM ACh and plotted against the
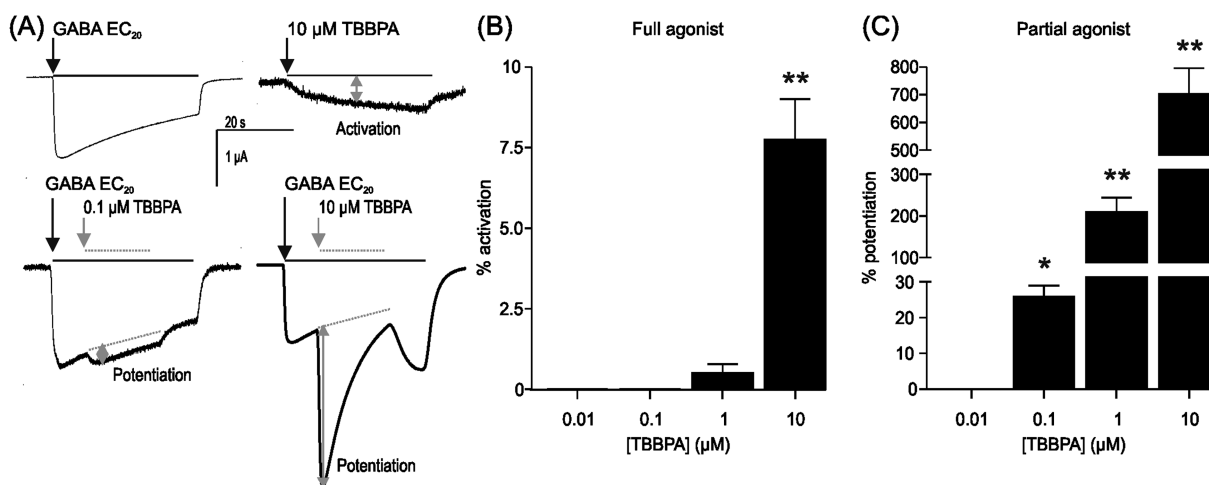

FIG. 1. Full and partial agonistic effects of TBBPA on human $\alpha_1\beta_2\gamma_2$ GABA$_A$ receptor. (A) Example recordings of ion currents evoked by TBBPA alone or coappled with GABA at EC$_{20}$. Application of TBBPA at 10μM resulted in activation of the GABA$_A$ receptor (upper right). When coappled with GABA at EC$_{20}$, TBBPA concentration dependently potentiate the GABA$_A$ receptor as is shown for 0.1μM (lower left) and 10μM TBBPA (lower right). Scale bar applies to all traces. (B) Bar graph demonstrating activation of the GABA$_A$ receptor evoked by TBBPA (LOEC = 10μM; $p < 0.001$). Activation is expressed as percentage of the maximum GABA-evoked response (1mM). (C) Bar graph demonstrating the concentration-dependent potentiation of GABA-induced responses by TBBPA (LOEC = 0.1μM; $p < 0.05$). Potentiation is expressed as percentage of the GABA-evoked response at EC$_{20}$. Bars represent mean ± SEM; $n = 4–5$ oocytes; *$p < 0.05$ versus control; **$p < 0.001$ versus control. The GABA concentration-response curve is shown in Supplementary figure S1.

agonist concentration to obtain a concentration-effect curve according to the Hill equation (see Supplementary figure S3). The Hill slope for the fitted ACh concentration-effect curve was 1.0 ± 0.1, and mean values for EC_{10} and EC_{50} amounted to 14 ± 2 and $139 \pm 17 \mu M$ ($n = 5$), which is in line with previous results (Hendriks *et al.*, 2010).

When human $\alpha_4\beta_2$ nACh receptor expressing oocytes were superfused with 10 or $100 \mu M$ TBBPA, no change in ion current was detected, demonstrating that TBBPA is not an agonist of the nACh receptor (Fig. 2A). However, as previously reported (Hendriks *et al.*, 2010), at low receptor occupancy, PCBs and PBDEs can affect the ACh-evoked current in a concentration-dependent manner. We therefore coapplied TBBPA with a low concentration of ACh ($10 \mu M$; ~EC_{10}). Although 0.1 and $1 \mu M$ TBBPA were without effect, exposure to $10 \mu M$ TBBPA resulted in a strong inhibition of the ACh-evoked ion current ($63 \pm 4\%$; $p < 0.001$; Figs. 2A and B). Comparable inhibitory effects of $10 \mu M$ TBBPA were observed when coexposed with ACh at 1 mM (see Supplementary figure S4). These measurements thus demonstrate that TBBPA acts as an antagonist of the human $\alpha_4\beta_2$ nACh receptor at a wide range of ACh concentrations.

TBBPA Dose Dependently Affects Basal and ACh-Evoked $[Ca^{2+}]_i$ in B35 Cells

To further investigate the mechanisms underlying the observed changes in cholinergic signaling, we used single-cell fluorescent Ca^{2+}-imaging. Fura-2 AM-loaded B35 neuroblastoma cells were used to determine acute effects of TBBPA exposure on Ca^{2+}-homeostasis and ACh-evoked increases in $[Ca^{2+}]_i$ as B35 cells have a high expression of calcium-permeable nACh receptors. B35 cells have a low basal $[Ca^{2+}]_i$ of $101 \pm 2 nM$ ($n = 88$), which rapidly and transiently increases

to $1.9 \pm 0.8 \mu M$ upon activation of nACh receptors for 15 s with $100 \mu M$ ACh (Fig. 3A). During a subsequent 5 min recovery period, $[Ca^{2+}]_i$ returned to near basal levels. Next, $[Ca^{2+}]_i$ remained low and comparable to control (0.1% DMSO) cells during a 20-min exposure to 0.1 and $1 \mu M$ TBBPA (0.1% DMSO: $163 \pm 7 nM$; $0.1 \mu M$ TBBPA: $190 \pm 17 nM$; $1 \mu M$ TBBPA: $154 \pm 12 nM$; Figs. 3A, B, and D). However, exposure to $10 \mu M$ TBBPA resulted in a strong and rather persistent increase in basal $[Ca^{2+}]_i$ ($1.4 \pm 0.1 \mu M$) after a delay of 1.0 ± 0.1 min (Figs. 3C and D).

Following the 20-min exposure to DMSO or TBBPA ($0.1–10 \mu M$), cells were challenged for a second time with $100 \mu M$ ACh (with or without TBBPA) to derive a net TR(see Materials and Methods section). For DMSO-exposed control cells, the second stimulation resulted in an increase in $[Ca^{2+}]_i$ up to $2.4 \pm 0.2 \mu M$, i.e., $135 \pm 16\%$ of the first stimulation (net TR; Fig. 3A). Although exposure to $0.1 \mu M$ TBBPA did not affect net TR compared with control cells, exposure to $1 \mu M$ TBBPA resulted in a significant reduction of the net TR ($44 \pm 7\%$ of control cells, $p < 0.001$; Figs. 3B and E). When cells were exposed to $10 \mu M$ TBBPA, the second ACh-evoked increase in $[Ca^{2+}]_i$ was virtually absent (Figs. 3C and E).

Because cells were continuously superfused with TBBPA-containing medium, possible accumulative effects of TBBPA in the cells were investigated in two separate sets of experiments. First, instead of 20-min exposure to $1 \mu M$ TBBPA, cells were superfused for 40 min prior to a second stimulation with $100 \mu M$ ACh. No significant change in TR was observed between the 20 and 40 min exposed cells ($44 \pm 7\%$ vs $53 \pm 7\%$ of control cells; $p > 0.05$; data not shown).

Second, cells were exposed for 20 min to $10 \mu M$ TBBPA without superfusion, i.e., after 5 min of baseline recording, saline-containing $10 \mu M$ TBBPA was bath-applied to the cells.
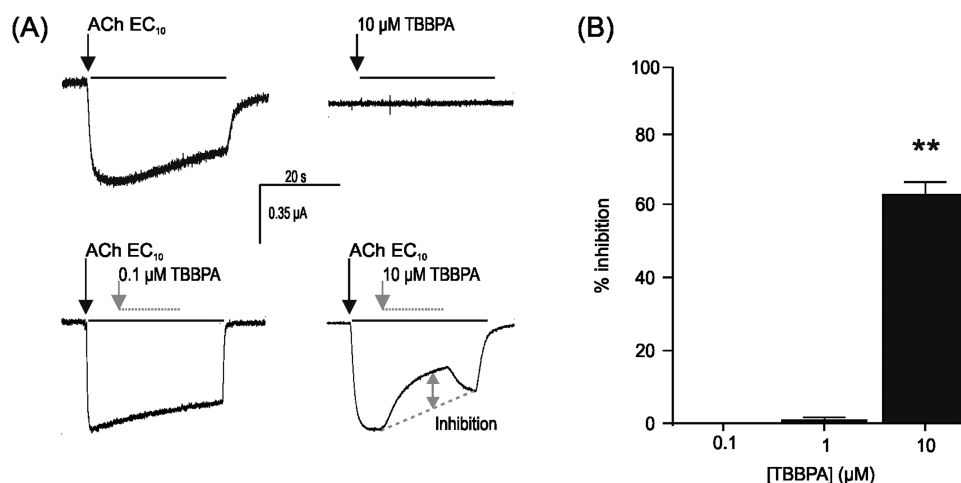
FIG. 2. Inhibitory effects of TBBPA on human $\alpha_4\beta_2$ nACh receptor activation. (A) Example recordings demonstrating TBBPA has no agonistic properties on the nACh receptor (upper right). During coapplication with ACh, no effect was observed for $0.1 \mu M$ TBBPA (lower left), though $10 \mu M$ TBBPA inhibited the ACh-evoked current (lower right). Scale bar applies to all traces. (B) Bar graph demonstrating the TBBPA-induced inhibition of ACh-evoked (EC_{10}) responses. Bars represent mean inhibition $\pm$ SEM; LOEC = $10 \mu M$ ($p < 0.001$); $n = 3–6$ oocytes; **$p < 0.001$ versus control. The ACh concentration-response curve is shown in Supplementary figure S3.
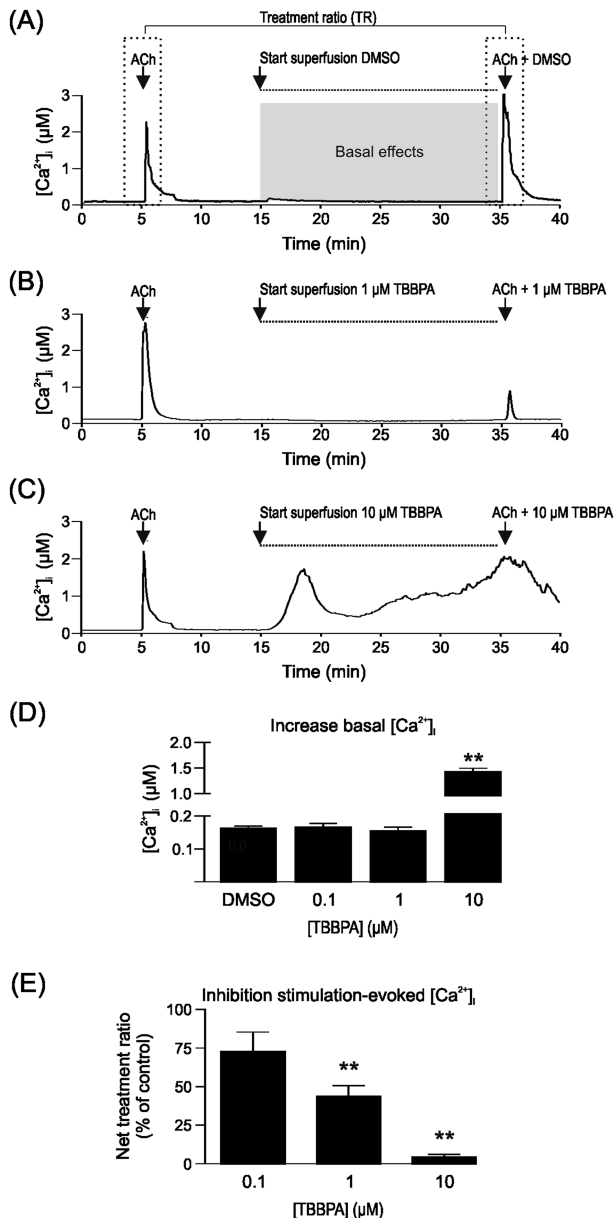
FIG. 3. TBBPA-induced effects on $[Ca^{2+}]_i$ in B35 cells. Example recordings of single-cell $[Ca^{2+}]_i$ imaging from individual B35 cells. In between two 15 s stimulations (100μM ACh), cells were exposed for 20 min to 0.1% DMSO (A) or different concentrations TBBPA (B and C), resulting in an increase in basal $[Ca^{2+}]_i$ and inhibition of the second ACh-evoked stimulation. Bar graphs illustrate the concentration-dependent TBBPA-induced increase in basal $[Ca^{2+}]_i$ (D) and inhibition of the stimulation-evoked increase in $[Ca^{2+}]_i$ expressed as a net TR normalized to DMSO-exposed control cells (E). $n = 29–88$ cells, $**p < 0.001$ versus control.

A significant increase in basal $[Ca^{2+}]_i$ was observed compared with control cells. However, no significant differences in basal $[Ca^{2+}]_i$ were observed between superfusion with 10μM TBBPA (1.4 ± 0.1μM) or bath application of 10μM TBBPA (1.8 ± 0.2μM; $p > 0.05$; data not shown).

Subsequently, cells were stimulated with 100μM ACh following 20-min superfusion or bath application. Again, no significant differences in $[Ca^{2+}]_i$ were observed between superfusion experiments (0.9 ± 0.1μM) and bath application experiments (1.2 ± 0.3μM; $p > 0.05$; data not shown). The TBBPA-induced inhibition of the ACh-evoked increase in $[Ca^{2+}]_i$ as well as the TBBPA-induced increase in basal $[Ca^{2+}]_i$ are thus rather independent of the exposure duration.

TBBPA Dose-Dependently Affects Basal and Depolarization-Evoked $[Ca^{2+}]_i$ in PC12 Cells

Because B35 cells lack functional VGCCs, single-cell fluorescent Ca²⁺-imaging of Fura-2 AM-loaded dopaminergic PC12 cells was used to study in more detail the effects of TBBPA on basal and depolarization-evoked calcium homeostasis. Comparable to B35 cells, PC12 cells have low basal $[Ca^{2+}]_i$ (112 ± 5nM; $n = 77$). Upon depolarization with 100mM K$^+$ for 15 s, $[Ca^{2+}]_i$ rapidly and transiently increases to 2.0 ± 0.1μM due to Ca²⁺ influx through VGCCs. During a 5-min recovery period, $[Ca^{2+}]_i$ returned to near basal levels and the cells were subsequently exposed to 0.1% DMSO (control) or TBBPA (0.1–10μM) for 20 min to measure effects on basal $[Ca^{2+}]_i$ (Fig. 4). Cells exposed to 0.1 and 1μM TBBPA have low basal $[Ca^{2+}]_i$ that is comparable to control cells (0.1% DMSO: 146 ± 3nM; 0.1μM TBBPA: 126 ± 9nM; 1μM TBBPA: 172 ± 11nM; Figs. 4A, B, and D). However, cells exposed to 10μM TBBPA display a strong transient increase in basal $[Ca^{2+}]_i$ up to 2.2 ± 0.4μM after a delay of 1.0 ± 0.1 min, that returns to near basal levels within minutes (Figs. 4C and D).

Following the 20-min exposure to DMSO or TBBPA (0.1–10μM), cells were challenged for a second time with 100mM K$^+$ to derive a net TR. In DMSO-exposed control cells, $[Ca^{2+}]_i$ increased to 1.2 ± 0.1μM during the second depolarization, i.e., 65 ± 3% of the first depolarization (net TR; Fig. 4A). Compared with control cells, 0.1μM TBBPA did not affect the net TR, whereas the net TR was significantly reduced in cells exposed to 1μM TBBPA (28 ± 4% of control cells, $p < 0.001$; Figs. 4B and E). The second depolarization-evoked increase in $[Ca^{2+}]_i$ was virtually absent in cells exposed to 10μM TBBPA (Figs. 4C and E).

To investigate the possibility of accumulation of TBBPA in the cells due to continuously superfusion, the cells were superfused for 40 min with 1μM TBBPA. Prolonged exposure did not result in a significant change of the TR compared with 20-min exposure (24 ± 3% after 40-min exposure vs 28 ± 4% after 20-min exposure; $p > 0.05$; data not shown). Also when the cells were exposed for 20 min to 10μM TBBPA via bath application, no significant difference in basal $[Ca^{2+}]_i$ was observed compared with cells exposed during 20 min with superfusion (1.8 ± 0.3μM without superfusion vs 2.2 ± 0.4μM with superfusion; $p > 0.05$; data not shown). The degree of inhibition of the depolarization-evoked increase in $[Ca^{2+}]_i$ was also comparable between superfusion experiments (0.3 ± 0.1μM) and bath application

experiments ($0.4 \pm 0.1\mu M$; $p > 0.05$; data not shown). The TBBPA-induced inhibition of VGCCs as well as the TBBPA-induced increase in basal $[Ca^{2+}]_i$ are thus rather independent of the exposure duration, in line with the results obtained in B35 cells.

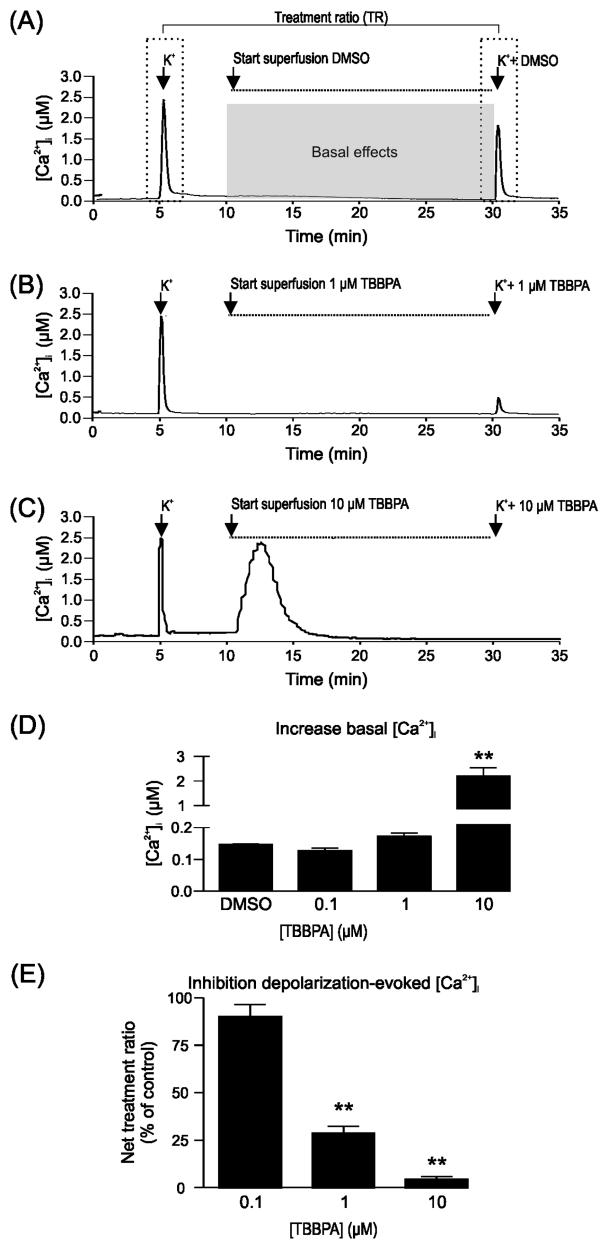**FIG. 4.** TBBPA-induced effects on $[Ca^{2+}]_i$ in PC12 cells. Example recordings of single-cell $[Ca^{2+}]_i$ imaging from individual PC12 cells. In between two 15 s depolarizations (100mM K^+), cells were exposed for 20 min to 0.1% DMSO (A) or different concentrations TBBPA (B and C), resulting in a concentration-dependent increase of basal $[Ca^{2+}]_i$ and inhibition of the second-evoked depolarization. Bar graphs illustrate the TBBPA-induced increase in basal $[Ca^{2+}]_i$ (D) and inhibition of the depolarization-evoked increase in $[Ca^{2+}]_i$ expressed as a net TR normalized to DMSO-exposed control cells (E). $n = 29$–77 cells, **$p < 0.001$ versus control.

TBBPA-Induced Increase in $[Ca^{2+}]_i$ Mainly Originates From Intracellular Stores

To investigate the mechanisms underlying the observed increases in basal $[Ca^{2+}]_i$, additional experiments were performed with PC12 cells under Ca^{2+}-free conditions. In the absence of extracellular Ca^{2+}, TBBPA ($10\mu M$) still induced an increase in $[Ca^{2+}]_i$, although the amplitude was significantly lower under these Ca^{2+}-free conditions ($312 \pm 18\%$ of DMSO control under Ca^{2+}-free conditions, $n = 71$, vs $1835 \pm 548\%$ of DMSO control under physiological Ca^{2+} conditions, $n = 47$, $p < 0.001$; Fig. 5A). The TBBPA-induced increase in $[Ca^{2+}]_i$ thus depends to a large degree on influx of extracellular Ca^{2+} but likely originates from the release of Ca^{2+} from intracellular stores, such as ER, mitochondria, nucleus, and secretory vesicles. We therefore depleted the ER and mitochondria of PC12 cells by pretreatment with $1\mu M$ TG and $1\mu M$ FCCP as described previously (Dingemans *et al.*, 2008). After depletion of ER with TG under Ca^{2+}-free conditions, $10\mu M$ TBBPA was still able to evoke an increase in basal $[Ca^{2+}]_i$, although the amplitude was significantly lower compared with normal and Ca^{2+}-free conditions ($191 \pm 11\%$ of control, $n = 29$, $p < 0.001$; Fig. 5B). Following depletion of both the ER and mitochondria by combined exposure to TG and FCCP prior to exposure to $10\mu M$ TBBPA, the increase in basal $[Ca^{2+}]_i$ was further attenuated and only slightly higher than in control cells ($125 \pm 2\%$ of control, $n = 44$, $p < 0.001$; Fig. 5B). The small remaining increase in basal $[Ca^{2+}]_i$ is probably due to release of Ca^{2+} from other intracellular stores, such as the nucleus and secretory vesicles.

Comparable effects were observed in B35 cells; in the absence of extracellular Ca^{2+}, $10\mu M$ TBBPA still induced a transient increase in $[Ca^{2+}]_i$ ($416 \pm 14\%$ of DMSO control under Ca^{2+}-free conditions, $n = 41$, vs $635 \pm 26\%$ of DMSO control under physiological Ca^{2+} conditions, $n = 45$, $p < 0.001$; Supplementary figure S5A). However, the TBBPA-induced fluctuations in $[Ca^{2+}]_i$ are absent under these Ca^{2+}-free conditions, indicating these are likely due to store-operated Ca^{2+} influx. After depletion of both ER and mitochondria under Ca^{2+}-free conditions prior to TBBPA exposure, the increase in basal $[Ca^{2+}]_i$ was decreased to only slightly higher than control cells ($148 \pm 5\%$ of control, $n = 39$, $p < 0.001$; Supplementary figure S5B), again indicating that the transient increase in $[Ca^{2+}]_i$ mainly originates from intracellular calcium stores.

Effects of TBBPA on Cell Viability, Caspase-3 Activity, and Oxidative Stress

To ensure that the observed effects are not confounded by acute cytotoxicity, B35 and PC12 cells were exposed to 1–$100\mu M$ TBBPA for 24 h, and cell viability was determined using a combined AB and NR assay. Exposure of B35 and PC12 cells to 1 and $10\mu M$ TBBPA did not affect cell viability. However, at $100\mu M$ TBBPA, a significant decrease in cell viability compared with control cells was observed in B35 cells
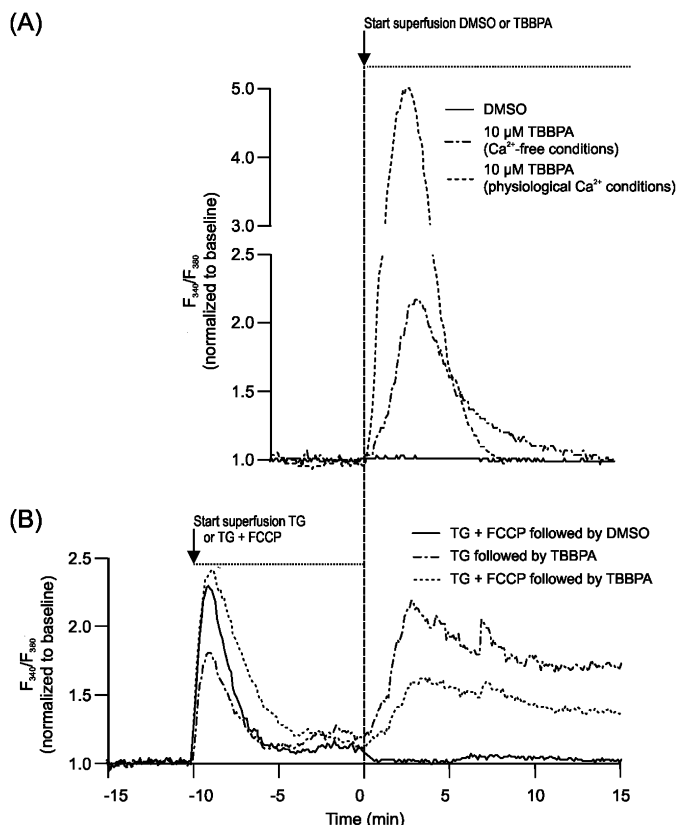
(A)

(B)

FIG. 5. TBBPA-induced increase of $[Ca^{2+}]_i$ is store-mediated. Example recordings of single-cell $[Ca^{2+}]_i$ imaging from individual PC12 cells under Ca^{2+}-free conditions illustrating that influx of extracellular calcium significantly contributes to the observed TBBPA-induced increase in basal $[Ca^{2+}]_i$ (A). The TBBPA-induced increase in basal $[Ca^{2+}]_i$ apparently originates from intracellular calcium stores as the increase in basal $[Ca^{2+}]_i$ is strongly reduced after depletion of mitochondria and ER by TG and FCCP (B). Comparable effects are observed in B35 cells, see Supplementary figure S5.

with the NR assay (70 ± 9%, $p < 0.001$; Fig. 6A) and in PC12 cells with both assays (AB: 50 ± 5%, $p < 0.001$; NR: 29 ± 5%, $p < 0.001$; Fig. 6B). Exposure to TBBPA for 24 h did already induce a clear increase in apoptosis-related caspase-3 activity at $\geq$ 10μM in PC12 cells (Supplementary figure S6), although lower concentrations were without effect.

Similarly, exposure to 1μM TBBPA did not increase ROS production in B35 or PC12 cells. In B35 cells, an increase in ROS production was observed at 10μM TBBPA only after 24 h (206 ± 6%, $p < 0.001$), whereas at 100μM, TBBPA increased ROS production already after 2 h compared with time-matched controls (148 ± 1%, $p < 0.001$), eventually amounting to 346 ± 5% following 24-h exposure (Fig. 7A). In PC12 cells, 10μM TBBPA also induced a modest increase in ROS production only after 24 h (123 ± 6%, $p < 0.001$). At 100μM TBBPA, ROS production was already significantly higher compared with time-matched controls following 1-h exposure (124 ± 1%, $p < 0.001$). ROS production increased further during the 24 h of exposure, eventually amounting to 167 ± 2% (Fig. 7B). The

combined results thus indicate that the observed acute TBBPA-induced neurotoxic effects *in vitro* at concentrations up to 10μM are not confounded by acute cytotoxicity.

DISCUSSION

Our results demonstrate that already a low concentration (0.1μM) TBBPA is able to act as a strong partial agonist of the human GABA$_A$ receptor (Fig. 1C). Furthermore, at higher concentrations TBBPA can also act as full agonist of the GABA$_A$ receptor (LOEC 10μM; Fig. 1B), whereas it acts as antagonist of the human $\alpha_4\beta_2$ nACh receptor (LOEC 10μM; Fig. 2B). These opposite effects of TBBPA, i.e., activation or potentiation of inhibitory GABA-mediated signaling and reduced excitatory ACh-mediated signaling, are of concern as they may add up *in vivo*. Moreover, comparable additive effects have been observed previously for PCB47 and 6-OH-BDE47 (Hendriks *et al.*, 2010). Interestingly, other studies also indicated the involvement of the cholinergic system in the neurotoxicity of chlorinated and brominated POPs (Eriksson *et al.*, 2001, 2006; Johansson *et al.*, 2008), suggesting that the cholinergic system may be a more general target for these compounds and that its modulation possibly underlies the neurobehavioral and neurodevelopmental effects induced by these compounds. Importantly, both GABA$_A$ and nACh receptors play an important role in long-term potentiation, synaptic plasticity, and brain development (D'Hulst *et al.*, 2009; Dwyer *et al.*, 2009). It should be noted that the GABA$_A$ receptor acts as an excitatory receptor during early brain development (D'Hulst *et al.*, 2009), which may explain some of the differences observed between behavioral studies following adult and neonatal exposure to TBBPA (Eriksson *et al.*, 2001; Nakajima *et al.*, 2009). Additionally, the discrepancy in behavioral effects after TBBPA exposure may be caused by the differences in animal species but probably also by differences in the timing of TBBPA treatment and the rather low retention time of TBBPA (Viberg and Eriksson, 2011).

The inhibitory effects of TBBPA on nACh receptors were confirmed in B35 cells expressing calcium-permeable nACh receptors (LOEC 1μM; Fig. 3E) using single-cell fluorescent $[Ca^{2+}]_i$ imaging. Importantly, our data also show that TBBPA ($\geq$ 1μM) reduced the depolarization-evoked increase in $[Ca^{2+}]_i$ in PC12 cells (Fig. 4E). This indicates that TBBPA is also a strong inhibitor of VGCCs, comparable with PBDEs (Dingemans *et al.*, 2011) and PCBs (Langeveld *et al.*, 2012). In neuronal cells, the main influx route of Ca^{2+} is via VGCCs. The rapid influx of Ca^{2+} can trigger various intracellular processes, including neurotransmitter release. In our PC12 cells, the L-type VGCC is the most abundant type, although N- and P/Q-type VGCCs both also account for ~20% of total calcium influx during depolarization (see also Dingemans *et al.*, 2009; Heusinkveld *et al.*, 2010). Since the depolarization-evoked increase in $[Ca^{2+}]_i$ was virtually absent in cells exposed
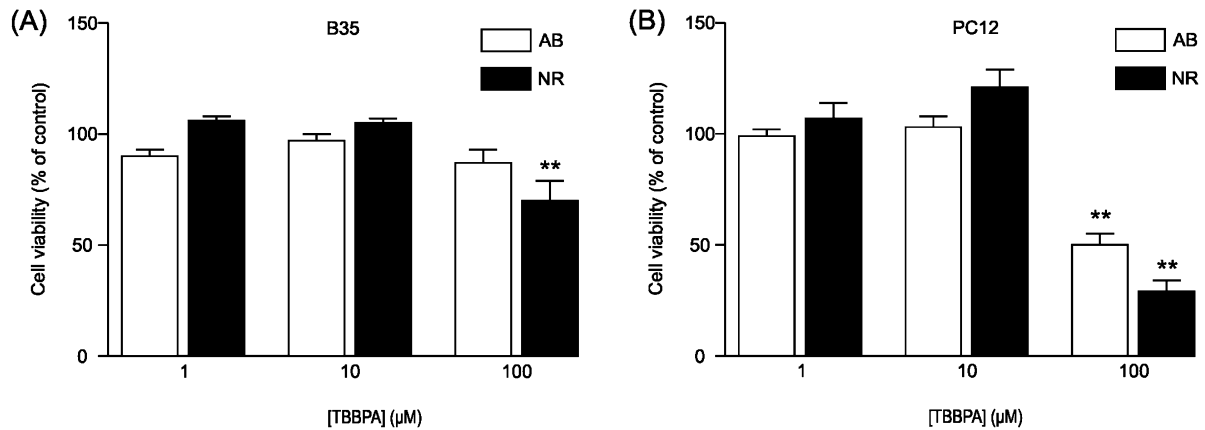
FIG. 6. Effects of 24-h exposure to TBBPA on cell viability in B35 and PC12 cells. Bar graphs, representing cell viability determined using a combined alamarBlue (AB; white bars) and Neutral Red (NR; black bars), demonstrate that TBBPA at 100μM decreases cell viability in B35 (A) and PC12 (B) cells. Bars represent mean cell viability compared with controls (set at 100%) ± SEM ($n = 27$–35 wells per concentration). **$p < 0.001$ versus control.

to 10μM TBBPA, the block of VGCCs is clearly not specific for a subtype of VGCCs, e.g., L-, N-, or P/Q-type. Moreover, the differences in LOECs between the increase in basal $[Ca^{2+}]_i$ (LOEC 10μM) and the decrease in ACh- and depolarization-evoked $[Ca^{2+}]_i$ (LOECs 1μM) indicate that the inhibition of nACh receptors and VGCCs is specific and independent of the foregoing increase of basal $[Ca^{2+}]_i$.

The observed robust TBBPA-induced ($\geq$ 10μM) increase in basal $[Ca^{2+}]_i$ in both B35 and PC12 cells (Figs. 3D and 4D) is in line with previous studies on cerebellar granule cells, granulocytes, and Sertoli cells (Ogunbayo and Michelangeli, 2007; Ogunbayo *et al.*, 2008; Reistad *et al.*, 2005, 2007) and indicates this is a general mechanism of action of TBBPA. In a separate set of experiments, we confirmed that influx of extracellular calcium significantly contributes to the observed TBBPA-induced increase in basal $[Ca^{2+}]_i$. However, the increase in basal $[Ca^{2+}]_i$ apparently originates from intracellular

calcium stores because the increase in basal $[Ca^{2+}]_i$ is strongly reduced after depletion of ER and mitochondria (Fig. 5 and Supplementary figure S5). Noteworthy, comparable store-mediated Ca^{2+} release was observed following exposure to PCBs and PBDEs (for reviews, see Dingemans *et al.*, 2011; Fonnum and Mariussen, 2009).

Interestingly, the observed ER-mediated increase in basal $[Ca^{2+}]_i$, as was observed following exposure to $\geq$ 10μM TBBPA, is an important trigger for induction of caspase activity and subsequent cell death (Orrenius *et al.*, 2011). Contrary, Reistad *et al.* (2007) showed that TBBPA (5μM) induces apoptotic cell death in cerebellar granule cells by a caspase-independent mechanism. It was suggested that caspase activity was suppressed by a TBBPA-induced increase in ROS production and that TBBPA-induced cell death was thus ROS-dependent. Our data (Fig. 7) confirm the TBBPA-induced increase in ROS production but also
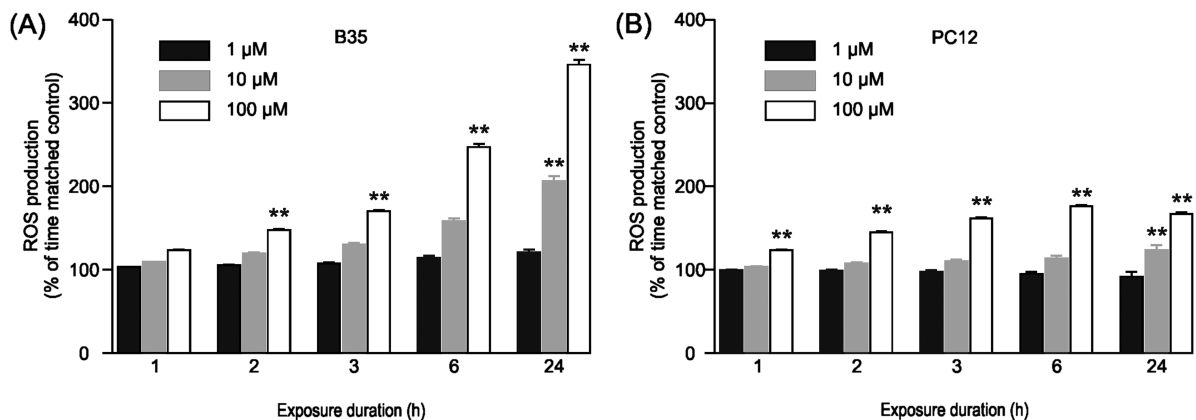

FIG. 7. Exposure to TBBPA increases ROS production over time in a concentration-dependent manner in B35 and PC12 cells. Bar graphs demonstrate that 10 (gray bars) and 100μM (white bars) TBBPA, but not 1μM (black bars), significantly increases ROS production in B35 (A) and PC12 (B) cells. Bars represent mean ROS production compared with time-matched controls (set at 100%) ± SEM ($n = 32$–111 wells per concentration). **$p < 0.001$ versus control.

revealed a TBBPA-induced ($\geq 10\mu M$) increase in caspase-3 activity in PC12 cells (Supplementary figure S6). Nonetheless, TBBPA-induced cell death was observed only at the highest concentration tested ($100\mu M$; Fig. 6) indicating that the specific neurotoxic effects of TBBPA at $\leq 10\mu M$ we report in this study are not confounded by acute cytotoxicity.

Neuronal circuits of mammals contain excitatory and inhibitory systems that should be in balance for normal (neuronal) development and functioning. In order to compare and integrate the observed adverse effects of TBBPA in this *in vitro* study, the effects on the different endpoints and corresponding LOECs were ordered according to an effect (target)—concentration ranking ranging from a high impact to a very low impact on normal neuronal development and function.

The observed strong partial agonistic effect of $0.1\mu M$ TBBPA on the inhibitory $GABA_A$ receptor is of major concern and suspected to potentially disturb normal neuronal development and function and is therefore ranked with a high impact. The observed inhibition of VGCCs and nACh receptors occurs only at higher concentrations (1 and $10\mu M$, respectively). Inhibition of VGCCs results in a reduced depolarization of the cell and less Ca^{2+} influx into the cell, thereby probably reducing, e.g., neurotransmitters secretion. Importantly, TBBPA has opposite effects on $GABA_A$ and nACh receptors, which may add up *in vivo* resulting in disequilibrium between excitatory and inhibitory systems. However, since these effects *in vitro* only occur at concentrations $\geq 1\mu M$, it is ranked with a moderate impact. The observed store-mediated disturbances in basal Ca^{2+} homeostasis observed in B35 and PC12 cells occur only at acute exposure to $10\mu M$, indicative for a low impact on normal neuronal development and function. The observed increases in ROS production and cytotoxicity only occur at high concentrations ($\geq 10\mu M$) and are therefore ranked as having a very low impact on normal neuronal development and function.

Clear epidemiological data on adverse effects of human (perinatal) TBBPA exposure are currently lacking, although TBBPA has been detected in human plasma (Thomsen *et al.*, 2002). Additionally, there are indications that acute exposure to TBBPA may cause behavioral disturbances (Nakajima *et al.*, 2009) and that developmental exposure can affect the cholinergic system in the neonatal mouse brain (Viberg and Eriksson, 2011). The margin of safety between the LOECs derived from our *in vitro* study and concentrations found in human serum of nonoccupational exposed adults are at least three orders of magnitude lower. However, of particular concern is the presence of high-concentrations TBBPA in breast milk (up to 4.11 ng/g lw) and cord serum (up to 103.52 ng/g lw) (Abdallah and Harrad, 2011; Cariou *et al.*, 2008; Shi *et al.*, 2009), which corresponds with ~2nM in blood (calculated using average human blood values). These cord serum values are not even two orders of magnitude below the LOECs of the most sensitive endpoint observed in this study (partial agonistic effect on the $GABA_A$ receptor, LOEC

100nM), indicating a possible risk for newborns and their developing brain. Although TBBPA is not a very stable compound (Birnbaum and Staskal, 2004), it is lipophilic and has a reported bioconcentration factor ranging from 20 to 230, which can explain the increasing TBBPA levels in humans despite its relatively short half-live (two days in human adults; Sjodin *et al.*, 2003). Moreover, our *in vitro* experiments focused on acute exposure, whereas human exposure is in general chronic with concentrations that could increase over time. Consequently, these findings should be taken into account for human risk assessment purposes, especially because several studies suggested that POPs, including PCBs and PBDEs, may exert additive neurotoxic effects (Antunes Fernandes *et al.*, 2010; Eriksson *et al.*, 2006; Gao *et al.*, 2009; Hendriks *et al.*, 2010).

In summary, this is the first study demonstrating differential effects of TBBPA at sub- and low-micromolar concentrations on human $GABA_A$ and nACh receptors. Importantly, TBBPA also inhibits VGCCs at $\geq 1\mu M$, resulting in decreased Ca^{2+} influx during neuronal activity and thus further inhibition of neuronal excitation. The observed increases in basal $[Ca^{2+}]_i$, ROS production, caspase-3 activity, and cell death were observed only at a higher TBBPA concentration ($\geq 10\mu M$) and may thus be less relevant for human risk assessment. TBBPA has several modes of action (potentiation and activation of $GABA_A$ receptors, inhibition of nACh receptors and VGCCs, ER-mediated Ca^{2+} release) that are shared by PCBs and PBDEs. TBBPA and other POPs may consequently interact at these targets, potentially causing additive or synergistic effects *in vivo*. Considering these effects and the wide application of BFRs, our findings underline the need to replace BFRs by safe(r) and less persistent alternatives.

SUPPLEMENTARY DATA

Supplementary data are available online at http://toxsci.oxfordjournals.org/.

REFERENCES

Abb, M., Stahl, B., and Lorenz, W. (2011). Analysis of brominated flame retardants in house dust. *Chemosphere* **85,** 1657–1663.

Abdallah, M. A., and Harrad, S. (2011). Tetrabromobisphenol-A, hexabromo-cyclododecane and its degradation products in UK human milk: Relationship to external exposure. *Environ. Int.* **37,** 443–448.

Antunes Fernandes, E. C., Hendriks, H. S., van Kleef, R. G., van den Berg, M., and Westerink, R. H. (2010). Potentiation of the human GABA_A receptor as a novel mode of action of lower-chlorinated non-dioxin-like PCBs. *Environ. Sci. Technol.* **44,** 2864–2869.

Birnbaum, L. S., and Staskal, D. F. (2004). Brominated flame retardants: Cause for concern? *Environ. Health Perspect.* **112,** 9–17.

Cariou, R., Antignac, J. P., Zalko, D., Berrebi, A., Cravedi, J. P., Maume, D., Marchand, P., Monteau, F., Riu, A., Andre, F., *et al.* (2008). Exposure assessment of French women and their newborns to tetrabromobisphenol-A: Occurrence measurements in maternal adipose tissue, serum, breast milk and cord serum. *Chemosphere* **73,** 1036–1041.

Covaci, A., Voorspoels, S., Abdallah, M. A., Geens, T., Harrad, S., and Law, R. J. (2009). Analytical and environmental aspects of the flame retardant tetrabromobisphenol-A and its derivatives. *J. Chromatogr. A* **1216,** 346–363.

Deitmer, J. W., and Schild, D. (2000). Calcium-Imaging, Protocolle und Ergebnisse. In *Ca²⁺ und pH, Ionenmessungen in Zellen und Geweben* (Anonymous, Ed.), p. 77. Spektrum Akademischer Verleger, Heidelberg, Germany.

de Wit, C. A., Herzke, D., and Vorkamp, K. (2010). Brominated flame retardants in the Arctic environment—Trends and new candidates. *Sci. Total Environ.* **408,** 2885–2918.

D'Hulst, C., Atack, J. R., and Kooy, R. F. (2009). The complexity of the GABA_A receptor shapes unique pharmacological profiles. *Drug Discov. Today* **14,** 866–875.

Dingemans, M. M., de Groot, A., van Kleef, R. G., Bergman, A., van den Berg, M., Vijverberg, H. P., and Westerink, R. H. (2008). Hydroxylation increases the neurotoxic potential of BDE-47 to affect exocytosis and calcium homeostasis in PC12 cells. *Environ. Health Perspect.* **116,** 637–643.

Dingemans, M. M., Heusinkveld, H. J., de Groot, A., Bergman, A., van den Berg, M., and Westerink, R. H. (2009). Hexabromocyclododecane inhibits depolarization-induced increase in intracellular calcium levels and neurotransmitter release in PC12 cells. *Toxicol. Sci.* **107,** 490–497.

Dingemans, M. M., van den Berg, M., and Westerink, R. H. (2011). Neurotoxicity of brominated flame retardants: (in)direct effects of parent and hydroxylated polybrominated diphenyl ethers on the (developing) nervous system. *Environ. Health Perspect.* **119,** 900–907.

Dwyer, J. B., McQuown, S. C., and Leslie, F. M. (2009). The dynamic effects of nicotine on the developing brain. *Pharmacol. Ther.* **122,** 125–139.

Eriksson, P., Fischer, C., and Fredriksson, A. (2006). Polybrominated diphenyl ethers, a group of brominated flame retardants, can interact with polychlorinated biphenyls in enhancing developmental neurobehavioral defects. *Toxicol. Sci.* **94,** 302–309.

Eriksson, P., Jakobsson, E., and Fredriksson, A. (2001). Brominated flame retardants: A novel class of developmental neurotoxicants in our environment? *Environ. Health Perspect.* **109,** 903–908.

Fonnum, F., and Mariussen, E. (2009). Mechanisms involved in the neurotoxic effects of environmental toxicants such as polychlorinated biphenyls and brominated flame retardants. *J. Neurochem.* **111,** 1327–1347.

Gao, P., He, P., Wang, A., Xia, T., Xu, B., Xu, Z., Niu, Q., Guo, L., and Chen, X. (2009). Influence of PCB153 on oxidative DNA damage and DNA repair-related gene expression induced by PBDE-47 in human neuroblastoma cells in vitro. *Toxicol. Sci.* **107,** 165–170.

Garcia, A. G., Garcia-De-Diego, A. M., Gandia, L., Borges, R., and Garcia-Sancho, J. (2006). Calcium signaling and exocytosis in adrenal chromaffin cells. *Physiol. Rev.* **86,** 1093–1131.

Greene, L. A., and Tischler, A. S. (1976). Establishment of a noradrenergic clonal line of rat adrenal pheochromocytoma cells which respond to nerve growth factor. *Proc. Natl. Acad. Sci. U.S.A.* **73,** 2424–2428.

Hendriks, H. S., Antunes Fernandes, E. C., Bergman, A., van den Berg, M., and Westerink, R. H. (2010). PCB-47, PBDE-47, and 6-OH-PBDE-47 differentially modulate human GABA_A and $\alpha_4\beta_2$ nicotinic acetylcholine receptors. *Toxicol. Sci.* **118,** 635–642.

Heusinkveld, H. J., Thomas, G. O., Lamot, I., van den Berg, M., Kroese, A. B., and Westerink, R. H. (2010). Dual actions of lindane (gamma-hexachlorocyclohexane) on calcium homeostasis and exocytosis in rat PC12 cells. *Toxicol. Appl. Pharmacol.* **248,** 12–19.

Heusinkveld, H. J., and Westerink, R. H. (2011). Caveats and limitations of plate reader-based high-throughput kinetic measurements of intracellular calcium levels. *Toxicol. Appl. Pharmacol.* **255,** 1–8.

Heusinkveld, H. J., and Westerink, R. H. (2012). Organochlorine insecticides lindane and dieldrin and their binary mixture disturb calcium homeostasis in dopaminergic PC12 cells. *Environ. Sci. Technol.* **46,** 1842–1848.

Hondebrink, L., Meulenbelt, J., Meijer, M., van den Berg, M., and Westerink, R. H. (2011a). High concentrations of MDMA ('ecstasy') and its metabolite MDA inhibit calcium influx and depolarization-evoked vesicular dopamine release in PC12 cells. *Neuropharmacology* **61,** 202–208.

Hondebrink, L., Meulenbelt, J., van Kleef, R. G., van den Berg, M., and Westerink, R. H. (2011b). Modulation of human GABA_A receptor function: A novel mode of action of drugs of abuse. *Neurotoxicology* **32,** 823–827.

IPCS (International Programme on Chemical Safety). (1995). *Environmental Health Criteria 172: Tetrabromobisphenol A and Derivatives.* World Health Organization, Geneva, Switzerland.

Johansson, N., Viberg, H., Fredriksson, A., and Eriksson, P. (2008). Neonatal exposure to deca-brominated diphenyl ether (PBDE 209) causes dose–response changes in spontaneous behaviour and cholinergic susceptibility in adult mice. *Neurotoxicology* **29,** 911–919.

Johnson-Restrepo, B., Adams, D. H., and Kannan, K. (2008). Tetrabromobisphenol A (TBBPA) and hexabromocyclododecanes (HBCDs) in tissues of humans, dolphins, and sharks from the United States. *Chemosphere* **70,** 1935–1944.

Langeveld, W. T., Meijer, M., and Westerink, R. H. (2012). Differential effects of 20 non-dioxin-like PCBs on basal and depolarisation-evoked intracellular calcium levels in PC12 cells. *Toxicol. Sci.* **126,** 487–496.

Law, R. J., Allchin, C. R., de Boer, J., Covaci, A., Herzke, D., Lepom, P., Morris, S., Tronczynski, J., and de Wit, C. A. (2006). Levels and trends of brominated flame retardants in the European environment. *Chemosphere* **64,** 187–208.

Nagayama, J., Tsuji, H., and Takasuga, T. (2000). Comparison between brominated flame retardants and dioxins or organochlorine compounds in blood levels of Japanese adults. *Org. Comp.* **48,** 27–30.

Nakajima, A., Saigusa, D., Tetsu, N., Yamakuni, T., Tomioka, Y., and Hishinuma, T. (2009). Neurobehavioral effects of tetrabromobisphenol A, a brominated flame retardant, in mice. *Toxicol. Lett.* **189,** 78–83.

Ogunbayo, O. A., Lai, P. F., Connolly, T. J., and Michelangeli, F. (2008). Tetrabromobisphenol A (TBBPA), induces cell death in TM4 Sertoli cells by modulating Ca²⁺ transport proteins and causing dysregulation of Ca²⁺ homeostasis. *Toxicol. In Vitro* **22,** 943–952.

Ogunbayo, O. A., and Michelangeli, F. (2007). The widely utilized brominated flame retardant tetrabromobisphenol A (TBBPA) is a potent inhibitor of the SERCA Ca2+ pump. *Biochem. J.* **408,** 407–415.

Orrenius, S., Nicotera, P., and Zhivotovsky, B. (2011). Cell death mechanisms and their implications in toxicology. *Toxicol. Sci.* **119,** 3–19.

Otey, C. A., Boukhelifa, M., and Maness, P. (2003). B35 neuroblastoma cells: An easily transfected, cultured cell model of central nervous system neurons. *Methods Cell Biol.* **71,** 287–304.

Peterman, P. H., Orazio, C. E., and Gale, R. W. (2000). Detection of tetrabromobisphenol A and formation of brominated [^{13}C]-bisphenol A in commercial drinking water stored in reusable polycarbonate containers. *ACS Div. Environ. Extended Abstr.* **40,** 431–433.

Reistad, T., Mariussen, E., and Fonnum, F. (2005). The effect of a brominated flame retardant, tetrabromobisphenol-A, on free radical formation in human neutrophil granulocytes: The involvement of the MAP kinase pathway and protein kinase C. *Toxicol. Sci.* **83,** 89–100.

Reistad, T., Mariussen, E., Ring, A., and Fonnum, F. (2007). *In vitro* toxicity of tetrabromobisphenol-A on cerebellar granule cells: Cell death, free radical formation, calcium influx and extracellular glutamate. *Toxicol. Sci.* **96,** 268–278.

Sellstrom, U., and Jansson, B. (1995). Analysis of tetrabromobisphenol A in a product and environmental samples. *Chemosphere* **91,** 49–58.

Shi, Z. X., Wu, Y. N., Li, J. G., Zhao, Y. F., and Feng, J. F. (2009). Dietary exposure assessment of Chinese adults and nursing infants to tetrabromobisphenol-A and hexabromocyclododecanes: Occurrence measurements in foods and human milk. *Environ. Sci. Technol.* **43,** 4314–4319.

Sjodin, A., Patterson, D. G., Jr, and Bergman, A. (2003). A review on human exposure to brominated flame retardants–particularly polybrominated diphenyl ethers. *Environ. Int.* **29,** 829–839.

Takigami, H., Suzuki, G., Hirai, Y., and Sakai, S. (2009). Brominated flame retardants and other polyhalogenated compounds in indoor air and dust from two houses in Japan. *Chemosphere* **76,** 270–277.

Thomsen, C., Lundanes, E., and Becher, G. (2002). Brominated flame retardants in archived serum samples from Norway: A study on temporal trends and the role of age. *Environ. Sci. Technol.* **36,** 1414–1418.

Udenfriend, S., Stein, S., Bohlen, P., Dairman, W., Leimgruber, W., and Weigele, M. (1972). Fluorescamine: A reagent for assay of amino acids, peptides, proteins, and primary amines in the picomole range. *Science* **178,** 871–872.

Viberg, H., and Eriksson, P. (2011). Differences in neonatal neurotoxicity of brominated flame retardants, PBDE 99 and TBBPA, in mice. *Toxicology* **289,** 59–65.

Westerink, R. H. (2006). Targeting exocytosis: Ins and outs of the modulation of quantal dopamine release. *CNS Neurol. Disord. Drug Targets* **5,** 57–77.

Westerink, R. H., and Ewing, A. G. (2008). The PC12 cell as model for neurosecretion. *Acta Physiol. (Oxf.)* **192,** 273–285.